

## Improvement of the Mechanical Properties of Sn-Ag-Sb Lead-Free Solders: Effects of Sb Addition and Rapidly Solidified

Mohammed, S. Gumaan <sup>1,2,\*</sup>, Esmail A. Ali <sup>2</sup>, Rizk M. Shalaby <sup>1</sup>, and Mustafa Kamal <sup>1</sup>

<sup>1</sup>*Metal Physics Lab., Physics Department, Faculty of Science, Mansoura University, Mansoura, Egypt.*

<sup>2</sup>*Basic Science Department, Faculty of Engineering, University of Science and Technology, Yemen.*

\* Author to whom correspondence should be addressed; E-Mail: [m.gumaan1@gmail.com](mailto:m.gumaan1@gmail.com)

*Article history:* Received 9 December 2016, Received in revised form 27 February 2017, Accepted 5 April 2017, Published 11 April 2017.

**Abstract:** The melt-spun processes of Sn-3.5 wt.%Ag and Sn-3.5 wt.%-Sbx ( $x = 0.1, 0.3, 0.5, 0.7$  and  $1.0$  wt.%) were analyzed using an x-ray diffractometer, a differential scanning calorimetry (DSC), and scanning electron microscopy (SEM). The results revealed that super saturated solid solution and intermetallic compounds (IMCs) were produced during melt-spun processes. The results revealed that there are more changes in thermal properties of these alloys due to structural reasons which are producing from micro-structural changes after Ag<sub>3</sub>Sn and AgSb Intermetallic compounds formation. The mechanical properties of the ternary Sn-Ag-Sb alloys have been improved after small alloying additions of Sb dramatically and rapidly solidified due to microstructure refining. The solder alloys have been withstanding creep deformation as show in their mechanical properties and creep results where the values of stress exponent and activation energy of Sn<sub>96</sub>-Ag<sub>3.5</sub>-Sb<sub>0.5</sub> were 7.87 and 66.51 KJ/mol respectively which indicate to dislocation climb controlled by dislocation pipe diffusion. It is known that even  $\geq 0.1$ wt% level additions of Sb have significant effects on the microstructure of Sn-Ag solder alloys. Sb suppresses the growth of  $\beta$ -Sn dendrites in favour of eutectic formation.

**Keywords:** Melt-spun ribbons; Intermetallic compound (IMC); microstructure

## 1. Introduction

Researchers already turned from the producing Sn-Pb solder alloys towards Pb-free solder alloys as a result of the Pb health problems. The development of Pb-free solders became one of the most important research areas of the electronic industry, Pb-free solders should be controlled by many factors such as acceptable cost, adequate span life and performance as a solder paste, good fatigue resistance, low melting temperature and no poorer than those of Sn-Pb solder, so tin is far utilize as one of the primary constituent in Pb-free solder alternatives; recent research has been mainly focused on eutectic Sn-Ag3.5 alloy due to its good mechanical properties and creep resistance, they got rid of the Pb health problems but some other problems such as high melting temperature, high cost and low interfacial bonding reliability have arisen. Some transition metals were added to these solders for improving the microstructural features of the Sn-Ag3.5 solders such as Cu, Co and Fe [1, 2]. Currently, SnAgCu (SAC) solders are most widely used for Pb-free applications.

In more papers published the formation of  $\text{Ag}_3\text{Sn}$  Intermetallic compound (IMC) enhances the creep resistance.  $\text{Ag}_3\text{Sn}$  intermetallic particles play two different roles. They may strengthen the alloy matrix and prevent the formation of large dislocation pile-ups at grain boundaries according to [3]. Adam J. Boesenberg et.al reported that the Al addition ( $>0.20\text{Al}$ ) to the (SAC3595) solders had good thermal stability and led to spontaneous of  $\text{Cu}_3\text{Sn}$  appear with  $\text{Ag}_3\text{Sn}$  hiding [4]. Other articles observe that the formation of  $\text{Ag}_3\text{Sn}$  IMC in  $\beta$ -Sn matrix, cause to increase the creep rate, thus decreasing the creep resistance due to micro cracks initiated and then failure process. Although the higher number of particles in a given matrix, the more matrix/intermetallics interfaces it contains, leading to a higher possibility of microcrack nucleation that can speed up the failure process. Adversely effecting of more amount of  $\text{Ag}_3\text{Sn}$  can occur on the plastic-deformation and restricts the formation of  $\beta$ -Sn phase [5]. Some alloying elements such as (Cu, Zn and Ni) have been added to the system to form ternary solders [6–8]. Rare researches using Sb as alloying element and used normal techniques, solders usually contain a maximum 0.5% Sb to eliminate the allotropic transformation. Hwa-Teng Lee et al [9]. reported that the in addition to SAS (Sn-Ag-Sb) alloys decreases the melting point and increased the pasty range temperature due to  $\text{Ag}_3\text{Sn}$  transformation to  $\text{Ag}_2(\text{In}, \text{Sn})$ . Good creep resistance and mechanical strength of eutectic Sn-Ag alloys occur when it's doped with Zn, Cu, or Sb due to refined microstructure. Enhancement of the creep resistance was occurred by Sb addition to Sn-Ag3.5 alloy, thus ternary alloys exhibited creep resistances higher than the binary Sn-Ag3.5 alloy [10]. Hwa-Teng Lee et al [11] reported that the fatigue life of the as-soldered joint increased with the amount of Sb additions due to less plastic strain the hardened solders produced. Binary phase diagram for Sn-Ag3.5 eutectic system indicates that there is little solid solubility of either minority constituent in the  $\beta$ -Sn

phase near room temperature, thus microstructural coarsening is appearing, since uniform phase distribution and small effective grain size forming have been attaining by quenching [12].

So, this paper is to solve the problem of creep deformation through refining  $\text{Ag}_3\text{Sn}$  IMC formed by Sb small additions to Sn-Ag3.5 alloy using rapidly solidified (melt-spinning technique) reaching to superior mechanical properties, and present new information concerned the structural stability, thermal behavior, mechanical properties and creep resistance obtained.

## 2. Materials and Methods

### 2.1. Sample Preparation

Six Pb-free alloys of compositions Sn96.5–Ag3.5–Sbx ( $x = \text{wt.}\%$  (0, 0.1, 0.3, 0.5, 0.7 and 1)) were prepared from pure Sn, Ag and Sb (purity > 99.99%). These alloys were putted in a porcelain crucible and melted by an electric furnace at 450 °C. After 25 min from heating the alloys become in a molten state then they are minutely agitated to increase the homogenization and again put in the furnace for 20 min. the molten alloys are shooting on the rotating copper wheel which has a linear speed of 31.4 m/s of the melt-spinning technique. The resulting alloys have long ribbons form of about 93  $\mu\text{m}$  in thickness and 4 mm width.

### 2.2. Sample Characterization

A variety of technique was used to characterize the crystallographic, and transformation features of the melt-spun ribbons Pb-free alloys including x-ray diffraction. The x-ray diffraction study was carried out using  $\text{CuK}\alpha$  radiation at room temperature. The microstructure analysis was carried out on a scanning electron microscope (SEM) of type (JEOL JSM-6510LV, Japan) operate at 30 kV with high resolution 3 nm. The melting temperature of these alloys was determined by differential scanning calorimetry, with a heating rate 10 k/min [13]. The mechanical properties were examined in air atmosphere with a dynamic resonance method [14–16]. The produced samples were tested in a Vickers microhardness tester, where a diamond pyramid indenter with square base is used and the Vickers hardness number is given by using  $H_v = 0.185F/d^2$  where F is the applied load in gram force (gf) and d, is the average diagonal length in mm. Micro-creep measurements as described elsewhere [17] were also carried out using a Vickers hardness tester using the different loads 10, 25 and 50 (gf) for dwell time up to 99 s.

## 3. Results and Discussion

### 3.1. Structural Analysis

In a detailed experimental study on structural properties where the rapid quenching of metallic alloys from melt was first carried out by Pol Duwez et al [18]. They found that the rapid quenching extends the solid solubility limits and produce non-equilibrium phase or amorphous alloys [19]. The patterns of X-ray diffraction obtained from the melt-spun ribbon for alloys are shown in fig.1. For  $\text{Sn}_{96.5}\text{-Ag}_{3.5}$  is shown in Fig.1a contains pure  $\beta\text{-Sn}$  phase and only two peaks for  $\text{Ag}_3\text{Sn}$  (IMC) phase embedded in the Sn matrix. For  $\text{Sn}_{96.4}\text{-Ag}_{3.5}\text{-Sb}_{0.1}$  alloy Fig.1b the number of peaks and intensity due to  $\text{Ag}_3\text{Sn}$  increases. According to the Hume-Rothery Rule, Sn atoms in the  $\text{Ag}_3\text{Sn}$  compounds can be easily replaced by Sb atoms to the phase transformation mechanism induced within the Sn-Ag-Sb system via increasing Sb addition can be summarized as:  $\text{Ag}_3\text{Sn} \rightarrow \text{AgSb}$ ,  $\text{AgSb}$  IMC phase indicated by a single line appeared at  $2\theta = 37.54^\circ$ ,  $2\theta = 37.59^\circ$  and  $2\theta = 37.62^\circ$  for  $\text{Sn}_{96.2}\text{-Ag}_{3.5}\text{-Sb}_{0.3}$  Fig.1c,  $\text{Sn}_{95.8}\text{-Ag}_{3.5}\text{-Sb}_{0.7}$  Fig.1e and  $\text{Sn}_{95.5}\text{-Ag}_{3.5}\text{-Sb}_1$  Fig.1f respectively, in addition to the presence of the above phases. It should be noted disappearance of the  $\text{AgSb}$  IMC phase in  $\text{Sn}_{96}\text{-Ag}_{3.5}\text{-Sb}_{0.5}$  Fig. 1d. Pure rhombohedra Sb phase only exist at 0.3 wt.% and 0.5 wt.% additions. It's found that generally the Sb addition enhancement the  $\text{Ag}_3\text{Sn}$  phase. No ternary phases are formed in the system nor  $\text{SnSb}$  phase formed. The details of the XRD analysis are shown in Table 1. Estimating of the particle size was implemented using Scherrer equation  $t = (0.9\lambda / B \cos\theta_B)$ , where: B is the broadening of diffraction line measured at half its maximum intensity (radians),  $\theta_B$  is the diffraction angle, t is the diameter of crystal particle and  $\lambda$  is the wavelength of x-ray. There are clearly decrease in the particle size of  $\beta\text{-Sn}$  as Sb increasing whereas fluctuation in values of  $\text{Ag}_3\text{Sn}$  IMC phase which is generally bigger than that of all other phases. The particle size of  $\text{AgSb}$  IMC phase is between 26.64nm-93.24nm, finally the lowest size was for Sb phase at 0.3 wt.% 13.01nm. Dominant phase is the phase of base metal. Refining of the particle size implemented by small amount additions of Sb where Sb suppresses the growth of coarse  $\beta\text{-Sn}$  dendrites in favor of eutectic formation. The variation of axial ratio c/a with different compositions is shown in table 1. Maximum value of axial ratio  $c/a = 0.5463$  at 0.5 wt% of Sb, due to expanding c-axis and contracting a-axis, this meaning decreasing in cell volume to become  $108.014\text{A}^\circ$ . From XRD analysis it's found the relatively refining of  $\text{Ag}_3\text{Sn}$  as alloying element (Sb) increased. Decreasing the number of atoms per cell volume which is due to existing point defects whereas maximum lattice distortion ( $\epsilon$ ) was at no Sb addition for Sn-matrix [20, 21].

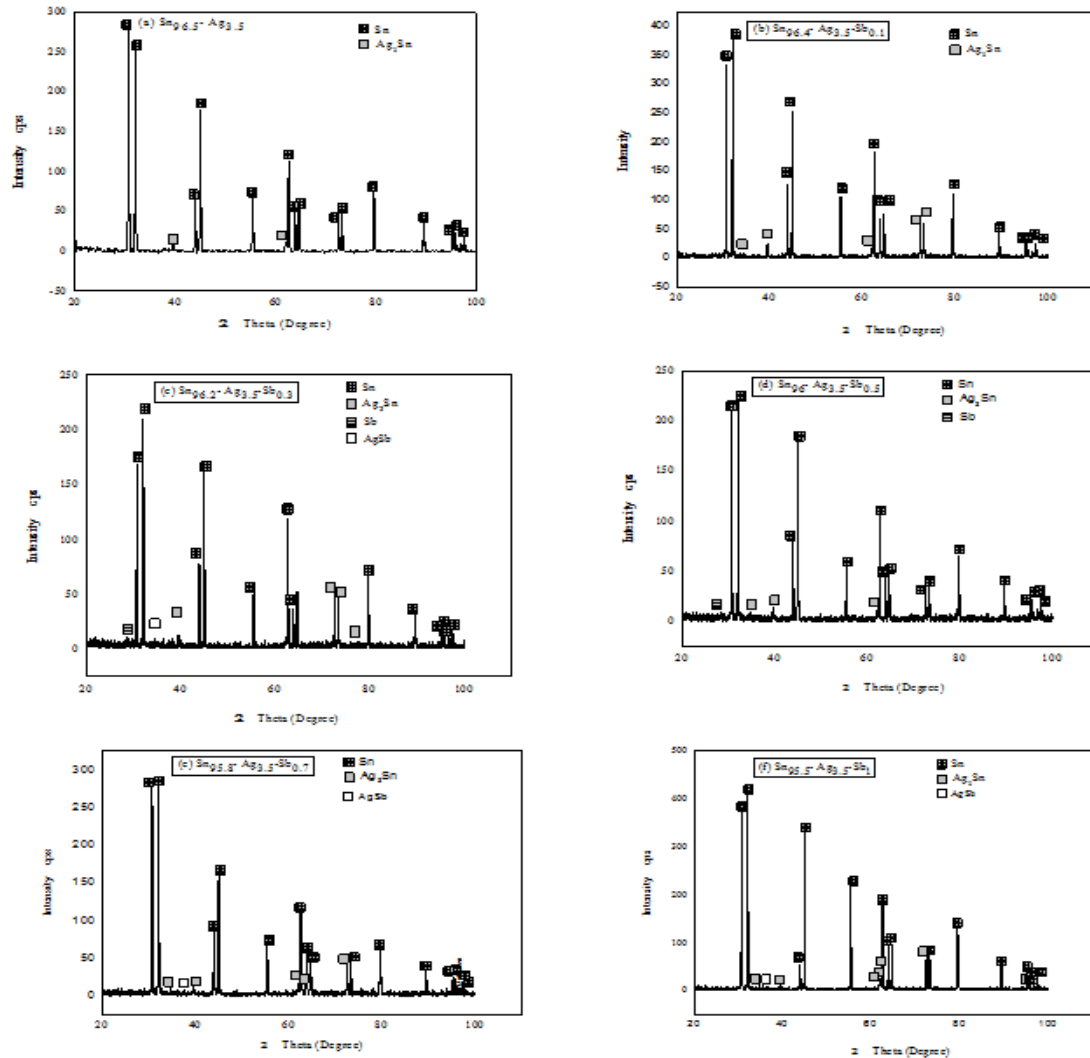


**Figure 1.** The XRD patterns of as quenched melt-spun alloys.

**Table 1.** The details of the XRD analysis

Solder	Phases	Particle size(nm)	a (Å)	c (Å)	(c/a) of $\beta$ -Sn	V (Å) <sup>3</sup>	N	$\epsilon \times 10^{-4}$
Sn96.5 – Ag3.5	$\beta$ -Sn	71.89	5.830	3.182	0.545	108.17	3.3	7.56
	Ag <sub>3</sub> Sn	98.41						4.09
Sn96.4 – Ag3.5 – Sb0.1	$\beta$ -Sn	70.42	5.833	3.178	0.544	108.16	2.4	6.56
	Ag <sub>3</sub> Sn	82.38						5.08
Sn96.2 – Ag3.5 – Sb0.3	$\beta$ -Sn	72.36	5.836	3.178	0.544	108.24	2.02	6.23
	Ag <sub>3</sub> Sn	96.78	-	-	-	-	-	4.16
	Sb	13.01	-	-	-	-	-	-
	AgSb	26.64	-	-	-	-	-	-
Sn96 – Ag3.5 – Sb0.5	$\beta$ -Sn	63.02	5.825	3.182	0.546	108.01	2.3	6.92
	Ag <sub>3</sub> Sn	96.44	-	-	-	-	-	4.41
	Sb	91.04	-	-	-	-	-	-
Sn95.8 – Ag3.5 – Sb0.7	$\beta$ -Sn	67.33	5.832	3.185	0.546	108.01	2.4	7.50
	Ag <sub>3</sub> Sn	87.73	-	-	-	-	-	5.21
	AgSb	93.24	-	-	-	-	-	-
Sn95.5 – Ag3.5 – Sb1	$\beta$ -Sn	66.74	5.826	3.184	0.546	108.08	2.4	6.45
	Ag <sub>3</sub> Sn	51.55	-	-	-	-	-	4.61
	AgSb	30.46	-	-	-	-	-	-

### 3.2. Stabilized and Refined Microstructure

Generally, Pb-free solder surfaces tend to be dull, matte, rough, and grainy, contrary to the typical shiny appearance of a Sn-Pb solder. The properties of the Sn-based solder matrix will be similar to the physical properties of tin, because the tin has relatively low solubility for alloying elements, the mechanical properties of the solders alloys are greatly affected by the microstructural changes [22]. The Sb element is preferred as alloying element in Sn96.5 – Ag3.5 due to solid solution hardening of Sb in the Sn matrix. The microstructures of Sn – Ag3.5 – Sb<sub>x</sub> ( x =0, 0.1, 0.3, 0.5, 0.7, and 1 wt%) are shown in fig.2. For Sn96.5 – Ag3.5, fig.2a the dark contrast dendritic globules are the  $\beta$ -Sn phase and the lighter contrast interdendritic regions contain the eutectic dispersion of Ag<sub>3</sub>Sn precipitates within a  $\beta$ -Sn matrix. The large grains microstructure coarsening with two-phase eutectic colony solidification structure occurred. Cracks propagated at the solder/IMC interface and through the solder. By eliminating the large Ag<sub>3</sub>Sn and uniform dispersion of Ag<sub>3</sub>Sn precipitates, the solidification microstructure of Sn96.5 – Ag3.5 alloy can be improved. With small amount of Sb addition, a more refined and uniform microstructure of Sn96.4 – Ag3.5 – Sb0.1 solder alloy has been obtained Fig.2b. Fig.2c, illustrated that there is a competition in the Sn-Ag-Sb system to form Ag<sub>3</sub>Sn vs AgSb or Sb and finest morphology has been occurred. At 0.5 wt% Sb fig.2d. the ductility in this ternary alloy is increased compared to that in the Sn96.5 – Ag3.5 binary alloy, thus increasing in creep resistance and activation energy. Increased ductility should result from a smaller effective grain size [12]. Approximately the microstructure and the formation of precipitate-free  $\beta$ -Sn dendritic globules has been completely suppressed. At 0.7wt% Sb fig.2e there are increasing in  $\beta$ -Sn dendrites and a void has been occurred. At 1wt% Sb fig.2f the cracks initiated. The microstructural changes that occur as a result of 0.1wt% Sb addition have a clear effect on the mechanical properties, as shown in the comparative creep curves in Fig.5. Approximately with Sb addition alloys have over 30 % more stress exponent and over 50 % in activation energy which due to microstructural modifications and the microstructure then become to resemble.

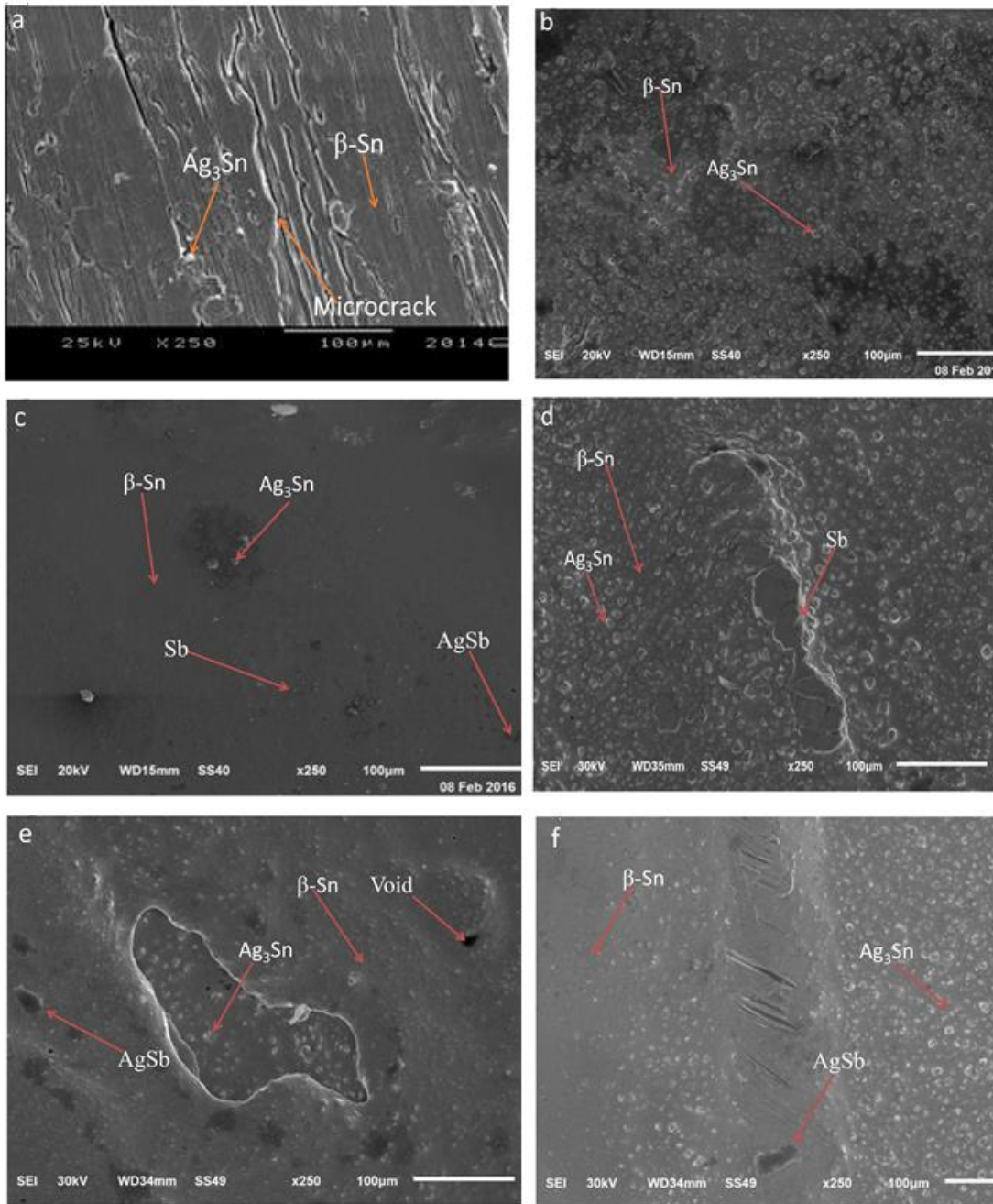


**Figure 2.** Micrographs of SEM for solder alloys: (a)  $\text{Sn}_{96.5} - \text{Ag}_{3.5}$  (b)  $\text{Sn}_{96.4} - \text{Ag}_{3.5} - \text{Sb}_{0.1}$  (c)  $\text{Sn}_{96.2} - \text{Ag}_{3.5} - \text{Sb}_{0.3}$  (d)  $\text{Sn}_{96} - \text{Ag}_{3.5} - \text{Sb}_{0.5}$  (e)  $\text{Sn}_{95.8} - \text{Ag}_{3.5} - \text{Sb}_{0.7}$  (f)  $\text{Sn}_{95.5} - \text{Ag}_{3.5} - \text{Sb}_1$ .

### 3.3. Melting and Thermal Behavior

The most challenge in Pb-free solders manufacturing is the high temperature, which it makes them difficult to be reflowed with devices on board and fabrication into existing physical forms of solder, i.e. wire, preforms, ribbon, spheres, powder, paste etc. Sb additions don't reduce the melt temperature of Sn-based solders; they go to enhance some properties. The optimal Sb content depends upon the particular properties of interest, to obtain the compromise of properties maximum limit of Sb addition is 1 wt.% which is provides a higher strength and

fatigue life compared to eutectic Sn-Ag without a detectable increase in melt temperature. The DSC curves obtained from the six alloys during heating with heating rate 10 K/min are shown in Fig.3. The melting point ( $T_m$ ), solidus temperature ( $T_s$ ), Liquids temperature ( $T_l$ ), enthalpy of fusion ( $\Delta H_f$ ), pasty range ( $\Delta T$ ), heat capacity ( $c_p$ ) and thermal energy for melting ( $q$ ) of these alloys were calculated in Table 2. There is only one endothermic peak for all solder alloys except at the first addition (0.1 wt.%) has been separated to two endothermic peaks due to  $\beta$ -Sn and  $Ag_3Sn$  phases.  $\Delta T$  is highly sensitive to the antimony content. Normally at eutectic composition  $\Delta T$  is zero, but in our case, it is not equal to zero, the reasons may be due to the effects of rapidly solidification from melt. The solidus temperature ( $T_s$ ) and liquids temperature ( $T_l$ ) behavior shows in fig.4 where the drop in ( $T_l$ ) to minimum value at 0.1 wt.% Sb and then slightly decrease to 1 wt.% Sb while the maximum value for ( $T_s$ ) at the same point which will release low pasty range value for this system as show in table 2. Other solder alloys  $> 0.1$  wt.% showing an increase up to  $14.86^\circ C$ . The different properties for solder alloy in this range temperature have been occurred which clarified it easy to form in different shapes. From table 2 it's clear that the ( $T_m$ ) and  $\Delta H_f$  values are sensitive to Sb atoms concentration, the maximum heat flow at 0.5 wt.% Sb which due to maximum enthalpy 66.52 (J/g). It's indicated that  $c_p$  is important factor for the solder material as intrinsic property. The lowest  $c_p$  was for an eutectic Sn<sub>96.5</sub>-Ag<sub>3.5</sub> alloy, suddenly  $c_p$  up to maximum value at 0.1 wt.% Sb which may be due to increasing  $Ag_3Sn$  content. After that continuous slightly decrease until 1 wt.% Sb as show in table 2. The low  $c_p$  means low energy needed for temperature changing hence lower cooling rate [23, 24]. By using this equation ( $q = m c_p \Delta t$ ) for the same mass (1.75 mg) of all solder alloys it's obvious that maximum energy needed for melting at 0.1 wt.% Sb and minimum energy needed at eutectic alloy as a function for  $Ag_3Sn$  content and their contribution (phase intensity) as show in XRD results.

**Table 2.** Thermal analysis

Solder	$T_s$ ( $^\circ C$ )	$T_l$ ( $^\circ C$ )	$T_m$ ( $^\circ C$ )	$\Delta H_f$ (J/g)	$\Delta T$ ( $^\circ C$ )	$c_p$ (J/g. $^\circ C$ )	q (J) for (1.75 mg)
Sn <sub>96.5</sub> -Ag <sub>3.5</sub>	212.5	237.5	217.4	1.391	25	0.0556	0.018
Sn <sub>96.4</sub> -Ag <sub>3.5</sub> -Sb <sub>0.1</sub>	215.18	219.27	216.96	31.58	4.09	7.721	2.526
Sn <sub>96.2</sub> -Ag <sub>3.5</sub> -Sb <sub>0.3</sub>	213.63	226.21	220.83	66.33	12.58	5.272	1.760
Sn <sub>96</sub> -Ag <sub>3.5</sub> -Sb <sub>0.5</sub>	213.12	227.98	222.22	66.52	14.86	4.476	1.505
Sn <sub>95.8</sub> -Ag <sub>3.5</sub> -Sb <sub>0.7</sub>	213.21	226.96	221.32	65.8	13.75	4.785	1.602
Sn <sub>95.5</sub> -Ag <sub>3.5</sub> -Sb <sub>1</sub>	213.4	226.83	222.38	58.78	13.43	4.376	1.473

### 3.3. Enhancement in Mechanical Properties

#### Young’s modulus and microhardness:

The microstructure is strongly influence the mechanical properties of a Pb-free solder, which is controlled by its cooling rate and alloying elements. The effective grain sizes and uniform dispersion of fine precipitates benefit the mechanical properties of solders and acquisition the ability to withstand the applied stresses. Mechanical observations reveal that Young’s modulus and hardness depend on concentration, distribution and size of Ag<sub>3</sub>Sn formed. Clear increasing in Young’s modulus and hardness values due to the addition Sb as shown in Table 3; however, the creep resistance was increased as shown in Fig. 5.

#### Stress exponent and activation energy of ordering:

Improvements in creep properties in the Pb-free alloys are desired to avoid rupture. The physical metallurgy of the solders is an important facet of mechanical deformation. Stress exponent strongly affected by the microstructural changes. Microstructural features such as grain boundaries and dislocation structures determine the strain response of the material to the applied stress. The creep tests were performed at room temperature. Deformation behavior of solder alloys was studied by micro-indentation creep experiments. In both alloys, micro-indentation creep rate was found to increase as a power-law function of indentation load. Fig.6 shows the plots of the quantity  $\ln \Delta c_p T^2$  against the  $(1/T) \times 10^{-3}$  give a straight line for each alloy. The slope of each straight line gives the activation energy (Q) of ordering for each alloy [25]. The exponents of the power-law were above 7 for lower creep rates. From this equation [26]:

$$n = \left[ \frac{\partial \ln \dot{d}}{\partial \ln H_V} \right]_d \dots\dots\dots(1)$$

where  $H_V$  is the Vickers hardness number,  $d$  is the indentation diagonal length, and  $\dot{d}$  is the rate of variation in indentation diagonal length, if  $\dot{d}$  is plotted against  $H_V$  on double logarithmic scale, a straight line would be obtained whose slope gives the stress exponent as show in fig.7. The observation that both creep resistance and activation energy increased with more uniform distribution and finer microstructure in SEM micrographs which is significant, due to high activation energy required to break the covalent bonds of IMCs in this solder alloy as shown in (energy needed for melting) work done for melting values in DSC data in table 2. Results indicate that at both stress levels, the activation energy increases with Sb addition. There is a strong indication that the improvement of creep behavior of Pb-free solder with Sb addition is due

to an increase in activation energy of ordering. Finally, the creep behavior of the Sn96.5 – Ag3.5 solder alloy has been improved due to the fine dispersive particles and the active properties of Antimony. It was found that the lowest creep for Sn96 – Ag3.5–Sb0.5 and Sn95.8–Ag3.5–Sb0.7. The stress exponent, activation energy and strain rate sensitivity values which are scheduled in table 4 indicates that dislocation climb controlled by dislocation pipe diffusion with stress exponent of  $\approx 7.8$ . Such change in creep behavior could be reflected by the microstructural changes observed in Fig.2, and XRD analysis Fig.1. However, the enhancement of creep resistance with increasing loading force is in good agreement with the result reported for Pb-free solders after Sb additions [8].

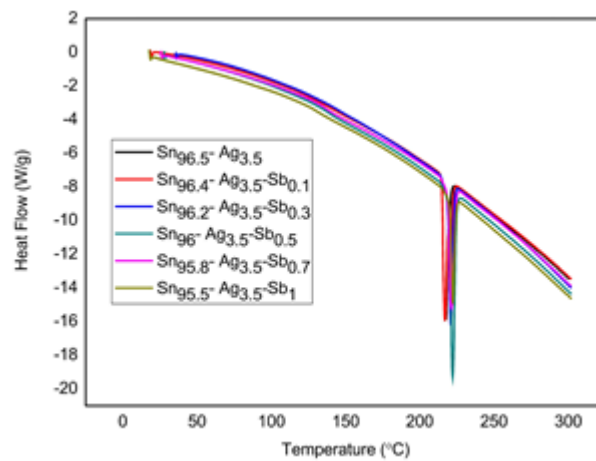


**Figure 3.** Differential Scanning Calimetry (DSC) melting curves for solder alloys

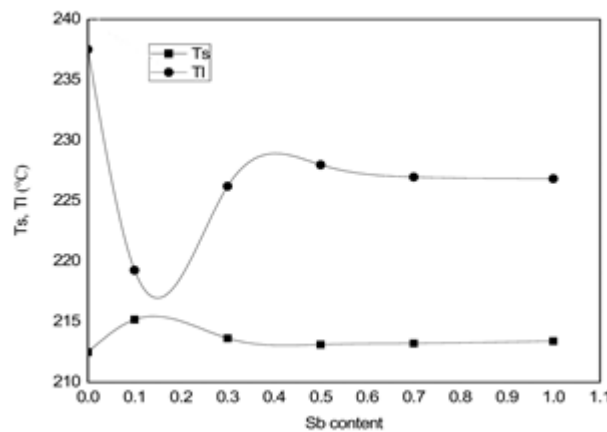


**Figure 4.** Variation of liquids temperature Tl and solidus temperature Ts with Sb addition

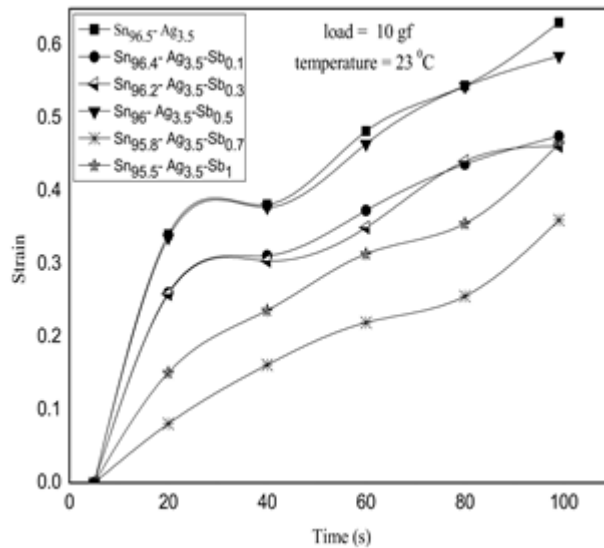


**Figure 5.** The creep behavior of as-quenched solder alloys

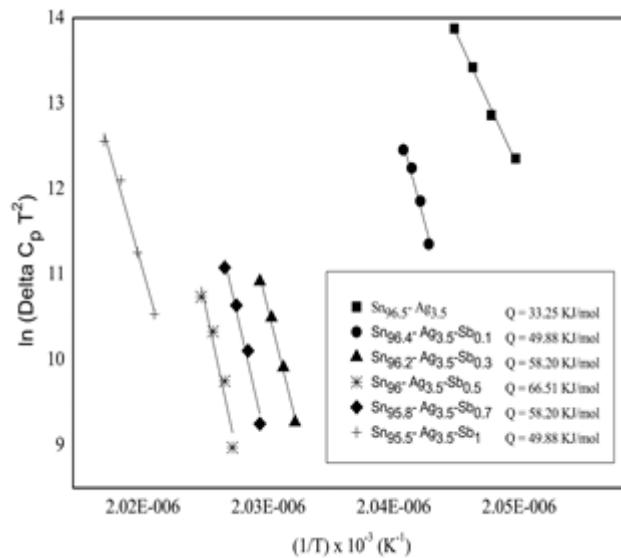


**Figure 6.** Relation between  $\ln\Delta c_p T^2$  values and  $(1/T) \times 10^{-3}$ .

Comparison of the indentation creep behaviors indicated that both Pb-free solder alloys have high creep resistance at room temperature, and the Sn96 –Ag3.5 –Sb0.5 has the highest creep resistance among the six solder alloys. Results from as-quenched samples showed that producing tended to reduce the indentation creep resistance of the alloy by promoting micro-crack spreading in the eutectic microstructure. The stress exponent  $n$  measurement was implemented at three different loads 10, 25, and 50 gf, the average is presented herein. As a compromise for thermal, mechanical, electrical and creep properties of the produced solder alloys, Sn96.5-Ag3.5 is a suitable alloy.

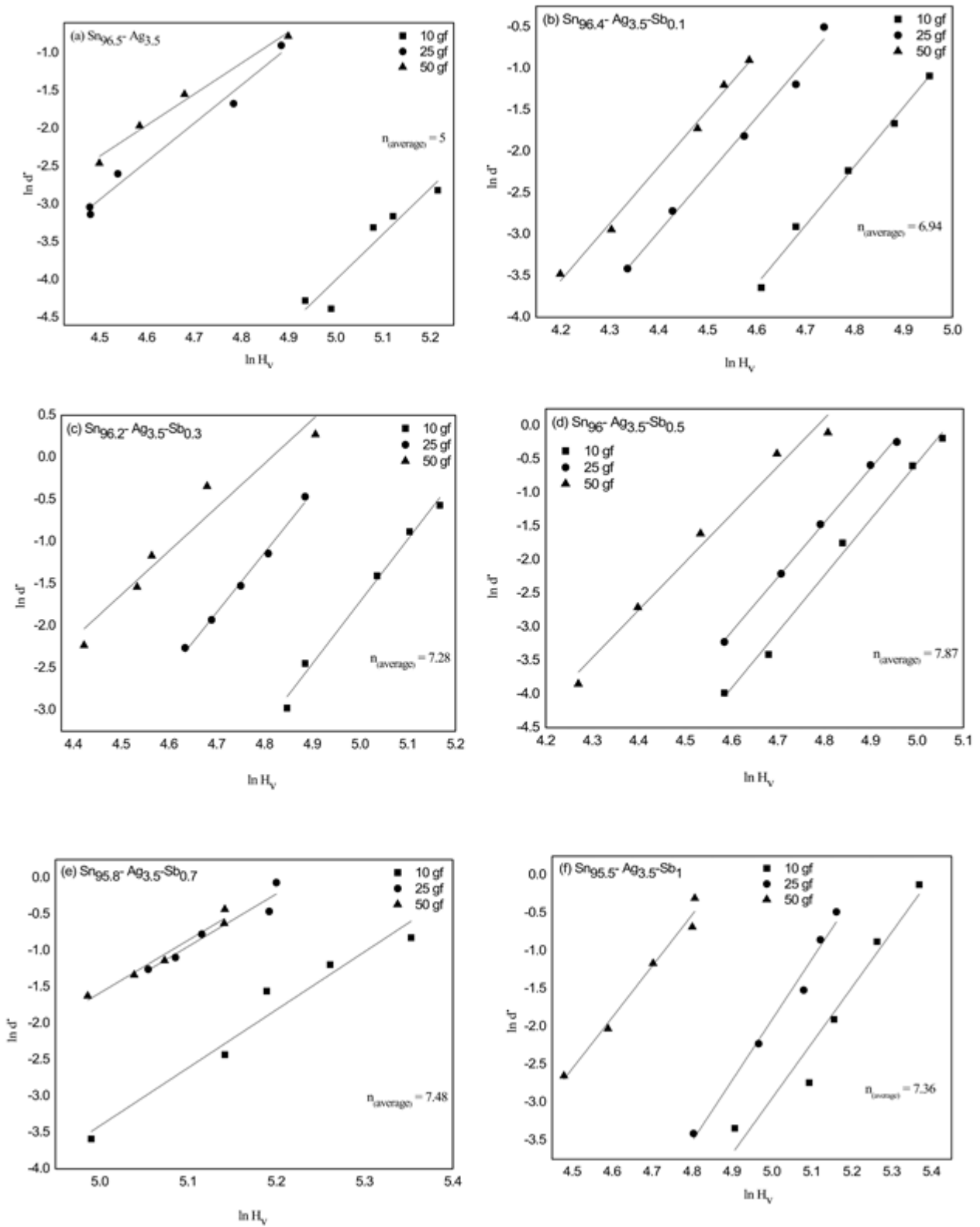


**Figure 7.**  $\ln - \ln$  plot of the rate of diagonal variation against the Vickers hardness numbers for solder alloys.

**Table 3.** Young's modulus and Vickers micro- hardness

Solder	E(Gpa)	Hv(M pa)
Sn96.5 – Ag3.5	212.5	237.5
Sn96.4 –Ag3.5 –Sb0.1	215.18	219.27
Sn96.2 –Ag3.5 –Sb0.3	213.63	226.21
Sn96 – Ag3.5 – Sb0.5	213.12	227.98

**Table 4.** Stress exponent (n), activation energy (Q) and strain rate (m)

Solder	n	Q(KJ/mol)	m
Sn96.5 – Ag3.5	5	33.25	0.166
Sn96.4 –Ag3.5 –Sb0.1	6.94	49.88	0.141
Sn96.2 –Ag3.5 –Sb0.3	7.28	58.20	0.136
Sn96 – Ag3.5 – Sb0.5	7.87	66.51	0.119
Sn95.8 –Ag3.5 –Sb0.7	7.48	58.20	0.131
Sn95.5 – Ag3.5 – Sb1	7.36	49.88	0.131

## 4. Conclusions

Enhancement, refine, and more uniform distribution for Ag<sub>3</sub>Sn were observed after Sb addition and rapidly solidified. Sb addition does not reduce the melt temperature of Sn-based solders, but enhance the mechanical properties. The values of stress exponent and activation energy of eutectic Sn-Ag after Sb addition were 7.87 and 66.51 KJ/mol respectively which indicates to dislocation climb controlled by dislocation pipe diffusion. Hardness and Young's modulus of solder depend on the size, distribution and the concentration of the Ag<sub>3</sub>Sn. As a compromise for suitable soldering temperature and time, lower energy needed for soldering process and more resistance deformations of the produced solder alloys, it's concluded that the Sn<sub>96</sub> –Ag<sub>3.5</sub>–Sb<sub>0.5</sub> is a suitable solder alloy for interconnects in electronic packages.

## References

- [1] B. A. Cook, I. E. Anderson, J. L. Haringa, and R. L. Terpstra, Effect of Heat Treatment on the Electrical Resistivity of Near- Eutectic Sn-Ag-Cu Pb-Free Solder Alloys, *Journal of Electronic Materials*, 2002, 31(11): 1190-1194.
- [2] M. Kamal and E. Gouda, Effect of zinc additions on structure and properties of Sn-Ag eutectic lead-free solder alloy, *J. Mater. Sci. Mater. Electron*, 2008, 19: 81-84.
- [3] C. M. L. Wu. Æ. Y. W. Wong, Rare-earth additions to lead-free electronic solders, *Lead-Free*

- Electron. Solder.*, 2006, (A Special): 77-91.
- [4] A. J. Boesenberg, I. E. Anderson, and J. L. Harringa, Development of Sn-Ag-Cu-X Solders for Electronic Assembly by Micro-Alloying with Al, *Journal of Electronic Materials*, 2012, 41(7): 1868-1881.
- [5] R. Kumar, Effect of Ag on Sn-Cu Lead Free Solders Effect of Ag on Sn-Cu Lead Free Solders, Department of Metallurgical and Materials Engineering National Institute Of Technology, *Rourkela*, 2014, 212: 1-62.
- [6] A. Gyenes, E. Nagy, P. Lanszki, and Z. Ga'csi, Investigation of Ni-Microalloyed Sn-0.5Cu Lead-Free Solders," *Adv. Mater. Res.*, 2015, (1120-1121): 466-472.
- [7] J. P. Jing, F. Gao, J. Johnson, F. Z. Liang, R. L. Williams, and J. M. Qu, Brittle Versus Ductile Failure of a Lead-Free Single Solder Joint Specimen Under Intermediate Strain Rate, *IEEE Trans. Components Packag. Manuf. Technol.*, 2011, 1(9): 1456-1464.
- [8] M. Pourmajidian, R. Mahmudi, A. R. Geranmayeh, S. Hashemizadeh, and S. Gorgan-nejad, Effect of Zn and Sb Additions on the Impression Creep Behavior of Lead-Free Sn-3.5Ag Solder Alloy, *J. Electron. Mater.*, 2016, (45)(1): 764-770.
- [9] H. Lee, F. Lee, T. Hong, and H. Chen, *En* ', 2008: 191-194.
- [10] R. Mahmudi, M. Pourmajidian, A. R. Geranmayeh, S. Gorgannejad, and S. Hashemizadeh, Materials Science and Engineering an Indentation creep of lead-free Sn-3.5Ag solder alloy: Effects of cooling rate and Zn / Sb addition, *Mater. Sci. Eng. A*, 2013, 565: 236-242.
- [11] H. Lee, H. Lin, C. Lee, and P. Chen, Reliability of Sn - Ag - Sb lead-free solder joints, *Mater. Sci. Eng. A*, 2005, 407: 36-44.
- [12] M. McCormack and S. Jin, Improved mechanical properties in new, Pb-free solder alloys, *J. Electron. Mater.*, 1994, 23(8): 715-720.
- [13] Y. A. GELLER and A. G. RAKHSHTADT, *Science of Materials, Sci. Mater.*, 1977, 138: 138-141.
- [14] J.M. Ide, *Rev. Sci, Instrum*, 1935, 6: 296.
- [15] S. Sppinert, and W.E. Teffit, *ASTM Proc*, 1961, 61:1221.
- [16] N. S. E. Schreiber, O.L. Anderson, *Elastic Constants and Their Measurements*, McGraw Hill, New York, 1973, p. 82.
- [17] T. El-Ashram and R. M. Shalaby, Effect of rapid solidification and small additions of Zn and Bi on the structure and properties of Sn-Cu eutectic alloy, *J. Electron. Mater.*, 2005, 34(2): 212-215.
- [18] P. Duwez, R. H. Willens, and W. Klement, Metastable electron compound in Ag-Ge alloys, *J. Appl. Phys.*, 1960, 31(6): 1137.
- [19] M. Kamal, A. El-Bediwi, and M. Jomaan, Rapid Quenching of Liquid Lead Base Alloys for High

Performance Storage Battery Applications, *IJET-IJENS*, 2012, 12 (6): 67.

- [20] B. D. Cullity, *Elements of X-ray Diffraction*. USA: Wesely, 1959.
- [21] G. K. WILLIAMSONt and W. H. HALLt, X-ray line broadening from filed aluminium and wolfram, *Acta Metall.*, 1953, 1(1): 22-31.
- [22] R. M. Shalaby, Indium, chromium and nickel-modified eutectic Sn-0.7 wt% Cu lead-free solder rapidly solidified from molten state, *J. Mater. Sci. Mater. Electron.*, 2015, 26(9): 6625-6632.
- [23] Y. K. Wu, K. L. Lin, and B. Salam, Specific Heat Capacities of Sn-Zn-Based Solders and Sn-Ag-Cu Solders Measured Using Differential Scanning Calorimetry, *Journal of Electronic Materials*, 2009, 38(2): 227-230.
- [24] J. N. Harris, MECHANICAL WORKING OF METALS, First edition, vol. 36. NEW YORK: MATERIALS SCIENCE AND TECHNOLOGY, 1983.
- [25] R. M. Shalaby, Correlation between thermal diffusivity and activation energy of ordering of lead free solder alloys Sn65 -X Ag25 Sb10 CuX rapidly solidified from molten state, 2005, 6: 187-191.
- [26] R. Roumina, B. Raesinia, and R. Mahmudi, Room temperature indentation creep of cast Pb-Sb alloys, *Scr. Mater.*, 2004, 51(6): 497-502.